Journal of Integrative Neuroscience

J. Integr. Neurosci. **2026**; 25(7): 50683
https://doi.org/10.31083/JIN50683

Original Research

Sarsasapogenin Improves Pathological Phenotypes in MPTP/MPP$^+$-Induced Parkinson's Disease Models: Synergistic Actions of Neurite Outgrowth, Neurotransmitter Modulation, and Anti-Inflammation

Wendi Deng[1], Jinfeng Hong[1], Weixia Li[1], Yi Zhang[1], Yongping Zhang[1], Zhiyou Yang[1,*]

[1]College of Food Science and Technology, Shenzhen Institute of Guangdong Ocean University, Guangdong Provincial Key Laboratory of Aquatic Product Processing and Safety, Guangdong Province Engineering Laboratory for Marine Biological Products, Zhanjiang Municipal Key Laboratory of Marine Drugs and Nutrition for Brain Health, Guangdong Ocean University, 524088 Zhanjiang, Guangdong, China
*Correspondence: zyyang@gdou.edu.cn (Zhiyou Yang)

Academic Editor: Zhi Dong Zhou
Submitted: 4 February 2026 Revised: 13 May 2026 Accepted: 20 May 2026 Published: 29 July 2026

Abstract

Background: Parkinson's disease (PD) is a prevalent neurodegenerative disorder hallmarked by progressive loss of midbrain dopaminergic (DA) neurons, neurite atrophy, neurotransmitter imbalance, and motor dysfunction. Therapeutic strategies targeting neuronal integrity and neuroinflammation hold translational value beyond conventional symptomatic therapies for PD. Sarsasapogenin, a natural steroidal saponin, exhibits documented neuroprotective properties in multiple neurological diseases. However, its therapeutic potential and underlying mechanisms in PD remain to be elucidated. **Methods:** The neuroprotective efficacy of sarsasapogenin was assessed in a subacute 1-methyl-4-phenyl-1,2,3,6-tetrahydropyridine (MPTP)-induced mouse PD model and 1-methyl-4-phenylpyridinium ion (MPP$^+$)-insulted primary cortical and dopaminergic neuronal cultures. Motor function was evaluated via a variety of behavioral tests. Survival of dopaminergic neurons was quantified using tyrosine hydroxylase (TH) immunostaining. Levels of monoamine neurotransmitters and their metabolites were measured using high-performance liquid chromatography (HPLC), while serum proinflammatory cytokines were determined using enzyme-linked immunosorbent assay (ELISA). Neurite outgrowth and neuronal viability were examined under both preventive and therapeutic treatment regimens *in vitro*. Potential molecular targets of sarsasapogenin were screened and identified via Drug Affinity Responsive Target Stability (DARTS) coupled with molecular docking. **Results:** Twenty-one-day sarsasapogenin intervention mitigated aberrant motor deficits in MPTP-treated mice, rescued TH$^+$ dopaminergic neurons in the substantia nigra, restored homeostasis of dopamine and norepinephrine, normalized the turnover of monoamines, and decreased peripheral levels of the proinflammatory cytokines tumor necrosis factor-α (TNF-α) and interleukin-1β (IL-1β). In primary neuronal cultures, sarsasapogenin significantly ameliorated MPP$^+$-triggered neurite atrophy and neuronal loss in both cortical and ventral mesencephalic dopaminergic neurons. DARTS screening combined with molecular docking identified serpin family H member 1 (Serpin) H1 as a candidate binding protein of sarsasapogenin, with a favorable binding affinity of −8.6 kcal/mol. **Conclusions:** Sarsasapogenin exerts comprehensive neuroprotective effects in preclinical PD models via synergistic modulation of dopaminergic neuronal survival, neurotransmitter balance, inflammatory inhibition, and neurite outgrowth. These findings highlight sarsasapogenin as a promising multi-target candidate for PD intervention, whereas the precise functional role of Serpin H1 in mediating its neuroprotective actions warrants further in-depth investigation.

Keywords: Parkinson's disease; sarsasapogenin; dopaminergic neurons; neurites; neurotransmitters; neuroinflammation

1. Introduction

Parkinson's disease (PD) is the second most prevalent neurodegenerative disorder globally, clinically manifested by progressive motor deficits including resting tremor, rigidity, bradykinesia, and postural instability, as well as non-motor symptoms such as cognitive impairment, anxiety, and sensory dysfunction [1,2]. The core neuropathological feature of PD is the selective and progressive degeneration of dopaminergic (DA) neurons within the substantia nigra, accompanied by striatal dopamine depletion and widespread disruption of neural circuits [3,4]. Mounting evidence has demonstrated that aberrant α-synuclein induces neurite atrophy and synaptic loss, thereby initiating and exacerbating the degeneration and apoptosis of dopaminergic neurons [5,6]. Notably, synaptic dysfunction and axonal degeneration are recognized as key pathological events in the early stage of PD [7,8]. Accordingly, therapeutic strategies targeting the preservation of neurite integrity and the promotion of neurite outgrowth hold great potential for the treatment of neurodegenerative disorders including PD [9,10].

Natural products have garnered growing interest as prospective candidates for neurodegenerative diseases intervention, owing to their favorable properties in neurite outgrowth and neuroprotection [11]. Sarsasapogenin, a steroidal saponin abundantly distributed in *Anemarrhena asphodeloides*, has been widely reported to exert diverse pharmacological properties, with neuroprotective and antidiabetic effects being the most well-characterized [12]. Preclinical studies have shown that sarsasapogenin promotes microglial polarization toward the beneficial M2 phenotype, alleviates neuronal damage, and ameliorates cognitive deficits in Alzheimer's disease and diabetes models [13,14]. Mechanistically, sarsasapogenin mitigates diabetes-associated memory impairment by suppressing the protease-activated receptor 1 (PAR-1)/nuclear factor kappa B (NF-κB)/NLR family pyrin domain-containing 1 (NLRP1) pathway and advanced glycation end-products and their receptor (AGEs/RAGE) axis [15]. Moreover, sarsasapogenin directly inhibits inflammatory responses in macrophages and adipocytes, thereby alleviating insulin resistance in high-fat diet-induced obese mice [16]. Despite these well-documented pharmacological activities, the potential neurite and neuronal protective effects of sarsasapogenin in PD remain to be elucidated.

In the current study, we explored the therapeutic effects of sarsasapogenin in 1-methyl-4-phenyl-1,2,3,6-tetrahydropyridine (MPTP)-induced PD mice and 1-methyl-4-phenylpyridinium ion (MPP^+)-insulted primary neuronal models. Its potential molecular target was further explored using Drug Affinity Responsive Target Stability (DARTS) combined with molecular docking simulation. Our findings demonstrated that sarsasapogenin alleviates core pathological phenotypes of PD via integrated effects on promoting neurite outgrowth, rescuing dopaminergic neurons, maintaining neurotransmitter homeostasis, and inhibiting inflammatory responses.

2. Materials and Methods

2.1 Reagents and Animal Treatment

A total of 44 Male C57BL/6 mice (3-month-old) were purchased from Zhuhai BesTest Bio-Tech Co., Ltd. (Zhuhai, China) and raised under specific pathogen-free conditions with a controlled environment (22 ± 1 °C, 50–60% relative humidity, 12 h light/12 h dark cycle). Standard chow and sterile water were available ad libitum throughout the experiment. Madopar tablets (24595, Roche, Shanghai, China) were obtained from Roche Pharmaceuticals Ltd. (Shanghai, China) via JingDong (JD) Pharmacy. 1-methyl-4-phenyl-1,2,3,6-tetrahydropyridine hydrochloride (MPTP·HCl; M0896, Sigma-Aldrich, Beijing, China) was purchased from Sigma-Aldrich (St. Louis, MO, USA). Sarsasapogenin (DZ0010, Chengdu Desite Bio-Tech, Chengdu, China) was acquired from Chengdu Desite Bio-Tech Co., Ltd. (Chengdu, China), with its chemical structure and purity (≥98%) confirmed by nuclear magnetic resonance (NMR) and high-performance liquid chromatography (HPLC) analyses, respectively.

Following 1-week of acclimatization, mice were randomly divided into five experimental groups (n = 8–9) and received corresponding interventions for 21 consecutive days. To ensure blinding during behavioral assessments, all drug solutions were prepared and coded by an independent researcher not involved in behavioral testing. The investigator responsible for drug administration and behavioral recordings remained blinded to group assignments until all data acquisition was completed. A subacute PD model was established by intraperitoneal (i.p.) injection of MPTP (30 mg/kg/day) for 5 consecutive days, a regimen widely adopted to elicit dopaminergic neurotoxicity, neurochemical disturbances, and characteristic motor deficits in mice [17,18]. Drugs were immediately orally administered (p.o.) after daily MPTP injection and continued for an additional 16 days. The five experimental groups were assigned as follows: (1) control group (0.5% hydroxypropyl methylcellulose (HPMC; HY-A0104, MCE, Shanghai, China) in saline, p.o. without MPTP treatment); (2) model group (0.5% HPMC in saline, p.o. with MPTP treatment); (3) madopar group (50 mg/kg, p.o.); (4) low-dose sarsasapogenin group (10 mg/kg, p.o.); (5) high-dose sarsasapogenin group (20 mg/kg, p.o.).

2.2 Behavioral Test

2.2.1 Open Field Test

The open-field test was conducted in a square arena (40 × 40 × 40 cm), with the floor divided into 25 equal grids (8 × 8 cm each). The central zone was defined as the 9 central squares (3 × 3 grid, covering 24 × 24 cm). Throughout the testing procedure, a lighting system (XR-XZ301, Xinruan Information Tech, Shanghai, China) was used to maintain uniform illumination at 60 lx to minimize environmental variability. Prior to formal testing, all mice underwent a 5 min habituation period to acclimate to the arena and reduce environmental stress. On the following day, each mouse was gently placed in the central grid of the arena and allowed to explore freely for 5 min. Between individual trials, the entire arena was thoroughly cleaned with 10% ethanol followed by water to eliminate residual olfactory cues. The total locomotor traveled distance and the number of entries into the central zone were automatically recorded and quantified using a video-tracking system (Xinruan Information Technology Co., Ltd.).

2.2.2 Rotarod Test

Motor coordination of mice was assessed using a rotarod apparatus (Model YLS-4C, Yiyan Technology Co., Ltd., Jinan, China). In the training session, mice were placed on the rotarod under a linear acceleration protocol (1 to 30 r/min over 300 s) for two consecutive days, with two trials per day. In the formal test, mice were subjected to three consecutive trials using the same acceleration pro-

tocol (1 to 30 r/min within 300 s). A 5-min inter-trial rest interval was provided to prevent fatigue. The falling latency was automatically detected and recorded by a photoelectric sensor system (YLS-4C, Yiyan Tech, Jinan, China). The latencies from the three test trials were averaged to obtain a single value per mouse.

2.2.3 Pole Test

The pole test apparatus was self-made, comprising a wooden pole (50 cm in height, 0.5 cm in diameter) wrapped in gauze to prevent the mice from slipping. A rubber ball was attached to the top of the pole to avoid mice's passive sitting behavior. Additionally, the base of the pole was padded with bedding to protect mice from injury in the event of falls. Prior to formal testing, all mice underwent adaptive training to acclimate to the apparatus. Each mouse received 3 consecutive training trials, with a 5 min interval between each trial. If a mouse failed to descend within 60 s, gentle guidance was provided to facilitate its downward movement. In the formal pole test, each mouse was located head-up on the rubber ball at the top of the pole. Two motor coordination parameters were recorded: turn time (defined as the duration for the mouse to rotate its head from an upward to a downward position) and total time (defined as the total elapsed time from placement at the top of the pole to reaching the base). Three valid trials were conducted for each mouse, and the mean value of the three trials was used for subsequent statistical analysis.

2.3 Sample Collection and Tissue Preparation

After completion of the behavioral tests, mice were deeply anesthetized via intraperitoneal injection of an anesthetic cocktail containing xylazine hydrochloride (23 mg/kg; X0059, TCI, Shanghai, China), zolazepam (15 mg/kg; HY-119146, MCE, Shanghai, China), and salbutamol hydrochloride (15 mg/kg; PHR3457, Sigma-Aldrich, St. Louis, MO, USA). Salbutamol hydrochloride was used as an adjuvant rather than a primary anesthetic agent, with the main purpose of mitigating anesthesia-induced bronchoconstriction and supporting respiratory function during the procedure [19]. Blood samples were collected from the retro-orbital sinus using sterile capillary tubes. Following a 30 min clotting period at room temperature, the sample was centrifuged at 2500 ×g for 15 min. The separated serum was harvested and stored at −80 ℃ until further analysis. For brain tissue collection, mice were transcardially perfused with ice-cold 0.1 M phosphate-buffered saline (PBS, pH 7.4) to remove circulating blood. Mice were deeply anesthetized and euthanized by transcardial perfusion under deep anesthesia. Then whole brains were subsequently dissected, fixed in 4% paraformaldehyde (PFA; P1110, Solarbio, Beijing, China) at 4 ℃ for 48 h, and then processed for subsequent histological experiments.

2.4 Immunohistochemical Staining

Coronal brain sections (15 μm thick) spanning the substantia nigra region (bregma: −3.08 to −3.88 mm) were prepared using a cryostat (KD-2950, Kedi, Jinhua, China). Sections were fixed in 4% PFA for 1 h at room temperature, followed by immunofluorescence staining with a mouse monoclonal anti-tyrosine hydroxylase (TH) primary antibody (1:200, MAB318, Sigma-Aldrich) overnight. Alexa Fluor 594-conjugated goat anti-mouse IgG secondary antibody (ab150116; Abcam, Cambridge, UK) was applied at a dilution of 1:400. 4',6-diamidino-2-phenylindole (DAPI; BOT-40043, Biomol, Hamburg, Germany) was used for nuclear counterstaining at a concentration of 1 μg/mL. Three anatomically matched sections per mouse were immunostained and captured using an ECHO Revolve fluorescence microscope (ECHO RVL-100-M, San Diego, CA, USA). Fluorescent images of TH^+ neurons were subsequently analyzed using ImageJ software (version 1.50i, National Institutes of Health, Bethesda, MD, USA). TH^+ neurons were manually counted following colocalization of TH- and DAPI-stained images and uniform fixation of image threshold values across all groups to standardize positive signal identification. Additionally, the mean fluorescence intensity of TH^+ signals was quantified using ImageJ after background subtraction.

2.5 High-Performance Liquid Chromatography (HPLC) Analysis

Midbrain tissue was selected for neurotransmitter analysis because it contains the cell bodies of dopaminergic neurons, allowing assessment of dopamine turnover and synthetic capacity, which complements the conventional measurement of striatal terminal dopamine (DA) depletion. The method used to measure neurotransmitters was based on that employed in a previous study [20]. Dissected midbrain tissues were weighed and homogenized on ice in lysis buffer containing 0.5 mmol/L disodium ethylenediaminetetraacetic acid (HY-W018746, MCE), 0.6 mol/L perchloric acid (109065, Sigma-Aldrich), and 0.1 g/L L-cysteine (HY-Y0337, MCE). The homogenate was centrifuged at 14,000 ×g for 15 min at 4 °C to remove cellular debris. The collected supernatant was mixed with an equal amount of perchloric acid precipitant containing 2 mmol/L disodium ethylenediaminetetraacetic acid and 1.2 mol/L dipotassium hydrogen phosphate, and incubated on ice for 10 min. The mixture was then centrifuged at 14,000 ×g for 15 min, and the supernatant was filtered through a 0.45 μm membrane. The concentrations of norepinephrine (NE), 5-hydroxytryptamine (5-HT), DA, and their respective metabolites [3-methoxy-4-hydroxyphenylglycol (MHPG), 5-hydroxyindoleacetic acid (5-HIAA), dihydroxyphenylacetic acid (DOPAC)] were quantified via an Agilent 1260 Infinity II system (Agilent Technologies, Santa Clara, CA, USA), coupled with a ZORBAX 300SB-C18 column (150 mm × 4.6 mm, 5 μm) and a 1260 infinity fluorescence de-

tector (excitation wavelength at 280 nm; emission wavelength at 330 nm). Calibration curves were constructed using authentic neurotransmitter and metabolite standards purchased from Sigma-Aldrich with the following catalog numbers: NE (N1100000), 5-HT (14927), DA (PHR1090), MHPG (H8759), 5-HIAA (H8876), DOPAC (11569), HVA (69673). The chromatographic conditions were set as follows: an isocratic elution mode with a mobile phase consisting of 0.05 M citrate-sodium acetate buffer (Phase A, pH 3.8; containing 0.5 mM sodium heptanesulfonate, 5 mM triethylamine, 0.5 mM disodium EDTA) and methanol (Phase B) at a ratio of 87:13 (v/v); flow rate was maintained at 1.0 mL/min, and injection volume was 10 µL.

2.6 Enzyme-Linked Immunosorbent Assay (ELISA)

Serum concentrations of pro-inflammatory cytokines [tumor necrosis factor-α (TNF-α), interleukin-1β (IL-1β)] and anti-inflammatory cytokines [transforming growth factor-β (TGF-β), IL-10] were quantified using commercial ELISA kits (TNF-α ELISA kit, MM-0132M1; IL-1β ELISA kit, MM-0040M1; TGF-β ELISA kit, MM-0135M1; IL-10 ELISA kit, MM-0176M1; Meimian, Yancheng, China), strictly following the manufacturer's instructions. All samples were assayed in duplicate wells, and the optical density values were measured at 450 nm using a microplate reader (ELx800, Biotek, Winooski, VT, USA).

2.7 Cell Culture, Cell Viability Assay, and Neurite Outgrowth Assessment

2.7.1 Primary Cortical and DA Neuronal Culture

Embryos were harvested from pregnant Institute of Cancer Research (ICR) mice (Zhuhai BesTest Bio-Tech, Zhuhai, China) at embryonic day 14 (E14). ICR mouse embryos were selected for primary neuronal culture due to their robust reproductive performance and high embryo yield, which are essential for obtaining sufficient viable neurons for large-scale *in vitro* experiments. Following removal of the dura mater, cerebral cortices or ventral mesencephalic tissues (enriched in dopaminergic neurons) were dissected and mechanically minced. Tissues were dissociated with 0.5% trypsin–EDTA (25300054, Gibco, Waltham, MA, USA) at 37 ℃ for 15 min, and the dissociated neurons were isolated and resuspended in Neurobasal medium (# 21103-049, Gibco) supplemented with 2% B27 supplement, 0.6% D-glucose, and 2 mM L-glutamine. Immunocytochemical characterization showed that $MAP2^+$ neurons accounted for ~75% of $DAPI^+$ cells in cortical cultures. At E14, ventral mesencephalic tissue was isolated to establish a mixed mesencephalic culture, which more closely mimics the *in vivo* cellular environment. TH^+ DA neurons represented ~4.4% of total $MAP2^+$ neurons. This culture system allows for the study of DA neurons in the presence of other neuronal and glial populations. Primary cultures were tested for mycoplasma contamination by Thermal Dropout Polymerase Chain Reaction (TD-PCR) and confirmed to be mycoplasma-free.

2.7.2 Primary Cortical Neuronal Viability and Neurite Outgrowth Assay

Cortical neurons were seeded into 8-well plates (80826, ibidi, Gräfelfing, Germany) at a density of 1.5×10^4 cells/cm^2. Following 3 days of *in vitro* culture, primary cortical neurons were co-treated with 1-methyl-4-phenylpyridinium ion (MPP^+; D048, Sigma-Aldrich) and sarsasapogenin for 48 h. All experiments were independently repeated three times. For cell viability assessment, Cell Counting Kit-8 (CCK-8; K1018, APExBIO, Houston, TX, USA) was added, followed by incubation at 37 ℃ for 3 h. The absorbance was measured at 450 nm using a microplate reader. For neurite density and length analysis, neurons were fixed with 4% PFA for 1 h at 25 °C, then subjected to immunofluorescence labeling with anti-β3-tubulin (1:200; sc-80005, Santa Cruz, Dallas, TX, USA). Alexa Fluor 594-conjugated goat anti-mouse IgG (1:400) was used as the secondary antibody. Nuclear counterstaining was performed with DAPI. Ten random fields of view per group were captured under an ECHO Revolve fluorescence microscope. Neurite length and neuronal numbers were quantitatively analyzed using the Neurite Tracer plugin of ImageJ software.

2.7.3 TH^+ DA Neurites Determination

To determine the optimal MPP^+ concentration and its cytotoxic effects on primary DA neurons, primary DA neurons were seeded into 48-well culture plates at a density of 5×10^4 cells/cm^2. After 4 days of *in vitro* culture, neurons were treated with MPP^+ at concentrations of 2, 5, 10 and 50 µM for 48 h.

To investigate the effects of sarsasapogenin on MPP^+-impaired neurite outgrowth in DA neurons, cells were seeded into 48-well culture plates at a density of 3×10^5 cells/cm^2. This seeding density was optimized based on preliminary experiments. In our initial MPP^+ concentration screening phase, a lower seeding density (5×10^4 cells/cm^2) resulted in an insufficient number of TH^+ DA neurons per microscopic field and excessively low axonal density, which compromised the accuracy and reproducibility of neurite outgrowth analysis. To ensure reliable quantification, the density was adjusted to 3×10^5 cells/cm^2, which guarantees approximately 10–20 TH^+ DA neurons per field for consistent and valid morphological assessment. Following 4 days of *in vitro* culture, neurons were treated with 2 µM MPP^+ for 48 h. Sarsasapogenin (0.1–1000 nM) was added as a either pre-treatment or post-treatment during the same 48-h period.

Subsequently, neurons were fixed with 4% PFA for 1 h at 25 °C and subjected to double immunofluorescence labeling with anti-microtubule-associated protein 2 (MAP2; 1:1000, ab32454, Abcam) and anti-TH (1:200; MAB318, Sigma-Aldrich), followed by Alexa Fluor 594 and 488 conjugated secondary antibodies (1:400; ab150116 and ab150077, Abcam). For each well, 4–5 (for MPP^+ con-

centration screening) or more than 7 (for sarsasapogenin intervention experiments) random fields were selected by moving the stage in a systematic grid pattern, avoiding well edges and areas with cell clumps or debris. Only isolated, non-overlapping TH^+/microtubule-associated protein 2 $(MAP2)^+$ neurons with clearly identifiable cell bodies and intact neurites were included. Fluorescent images were captured and neurites were quantified using the Neurite Tracer plugin of ImageJ software.

2.8 Drug Affinity Responsive Target Stability (DARTS)

Primary DA neurons were isolated from E14 ICR mice and cultured in 10-cm dishes at a seeding density of 1.82×10^5 cells/cm^2 for 4 days. Cells were lysed using M-PER mammalian protein extraction reagent (78501, Thermo Scientific), supplemented with 1× protease inhibitor cocktail (78429, Thermo Scientific). Equal aliquots of cell lysate (10 µg total protein per sample) were incubated with sarsasapogenin (dissolved in dimethyl sulfoxide (DMSO)) at final concentrations of 10 µM or 100 µM for 60 min at room temperature (RT). The lysate-drug mixtures were then proteolyzed with 1 µg thermolysin (P1512, Sigma-Aldrich) in the reaction buffer for 25 min at 37 °C, and proteolysis was terminated by adding 0.5 M EDTA (pH 8.0) at a ratio of 1:10 (v/v). All samples were separated by sodium dodecyl sulfate–polyacrylamide gel electrophoresis (SDS-PAGE), and protein bands were visualized using the Pierce™ Silver Stain Kit (24612, Thermo Scientific). The experiment was conducted in two independent biological replicates. Protein bands showing enhanced stability in sarsasapogenin-treated groups compared with vehicle-treated controls were excised from gels and submitted for nano-liquid chromatography-tandem mass spectrometry (nano LC-MS/MS) analysis.

2.9 Molecular Docking

Molecular docking simulations were carried out using AutoDock Vina 1.2.6 (The Scripps Research Institute, La Jolla, CA, USA). The optimal binding conformer was selected according to the highest clustering frequency and the most favorable binding affinity. The three-dimensional (3D) structure of Serpin H1 was retrieved from the RCSB Protein Data Bank (RCSB PDB; https://www.rcsb.org/) and verified via the UniProt Knowledgebase (UniProtKB; https://www.uniprot.org/uniprotkb). The 3D chemical structure of sarsasapogenin was obtained from the PubChem database (https://pubchem.ncbi.nlm.nih.gov/). Binding interactions between sarsasapogenin and Serpin H1 were visualized and analyzed using PyMOL 3.1 (Version 3.1.8, Schrodinger, New York, NY, USA) for 3D structural rendering and Discovery Studio 2019 (DS 2019; Dassault Systèmes, San Diego, CA, USA) for two-dimensional (2D) interaction diagram generation.

2.10 Statistical Analysis

All statistical analyses were performed using GraphPad Prism 9.0 (GraphPad, San Diego, CA, USA). Data are expressed as mean ± SEM. Comparisons among multiple groups were conducted using one-way ANOVA followed by Tukey's multiple comparisons test. Two-way ANOVA was used for experiments involving two independent variables, followed by Tukey's multiple comparisons test when appropriate. Unpaired two-tailed Student's *t*-tests were used for comparisons between two groups. Exact F values, degrees of freedom, and adjusted *p* values are reported in the figure legends. A p-value < 0.05 was considered statistically significant.

3. Results

3.1 Sarsasapogenin Ameliorates MPTP-Induced Hyperactivities in Mice

MPTP is a well-established neurotoxin widely used to establish PD mouse models [21]. In the present study, we established a subacute PD model by intraperitoneally injecting mice with MPTP at a dose of 30 mg/kg for 5 consecutive days. Behavioral assessments, including the open-field test, rotarod test, and pole test, were performed to comprehensively evaluate motor function and anxiety-like behaviors in mice (Fig. 1A).

Following MPTP induction, mice in the vehicle (Veh) and all drug-treated groups exhibited a significant initial weight loss. However, body weight gradually recovered and slightly increased after 5 days of MPTP administration, and no statistically significant differences were observed among the Veh, madopar (Mad), low-dose sarsasapogenin (Sar-L), and high-dose sarsasapogenin (Sar-H) groups throughout the experimental period (Fig. 1B). In the open-field test, compared with the Cont (Control) group, the Veh group showed a significant increase in total locomotor distance and a higher number of entries into the central zone, which reflects hyperactive behaviors and locomotor dysfunction. Treatment with madopar or sarsasapogenin significantly reduced both locomotor distance and the number of central zone entries (Fig. 1C). In the rotarod test, the Veh group exhibited a non-significant trend toward increased fall latency compared with the Cont group (Fig. 1D). Although this might appear to suggest improved motor performance, such a trend has been reported in some subacute MPTP paradigms and is thought to reflect compensatory behavioral responses rather than genuine motor enhancement [22]. In the pole test, no significant differences were detected among all groups in either turn latency (Fig. 1E) or total descent time (Fig. 1F).

To further assess the protective effect of sarsasapogenin on DA neurons, immunofluorescence staining was performed using TH, a specific marker for DA neurons, to evaluate the survival of DA neurons in the substantia nigra pars compacta (SNpc). Quantitative analysis demonstrated a significant reduction in the number of TH^+ DA neurons

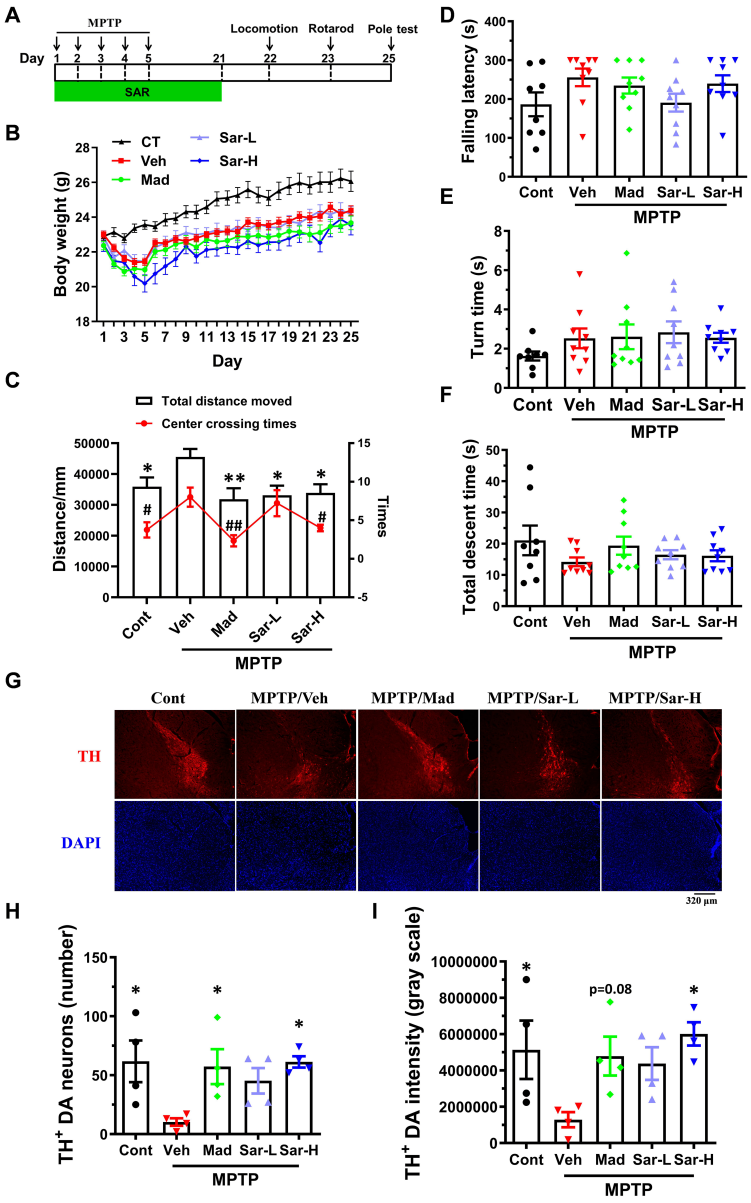

Fig. 1. Sarsasapogenin modulates motor behavior and protects dopaminergic neurons in MPTP-induced PD mice. (A) Schematic of the experimental protocol. Male C57BL/6 mice (3 months old, n = 8–9) were intraperitoneally injected with MPTP (30 mg/kg) to establish the PD model, followed by intragastric administration of low-dose sarsasapogenin (10 mg/kg), high-dose sarsasapogenin (20 mg/kg), or Madopar (50 mg/kg) for 21 consecutive days. (B) Changes in body weight of mice during drug treatment. (C) Total distance moved and center crossing times in the open field test (Two-way ANOVA, Interaction, F (4, 78) = 4.108, $p = 0.0042$, $\eta p^2 = 0.156$; Row Factor, F (4, 89) = 4.113, $p = 0.0042$, $\eta p^2 = 0.156$ and Column Factor, F (1, 89) = 645.6, $p < 0.0001$, $\eta p^2 = 0.879$). (D) Falling latency in the rotarod test (One-way ANOVA, F (4, 39) = 2.265, $p = 0.0762$, $\eta p^2 = 0.162$). (E) Turn time in the pole test (One-way ANOVA, F (4, 39) = 1.165, $p = 0.3389$, $\eta p^2 = 0.094$). (F) Total descent time in the pole test (One-way ANOVA, F (4, 39) = 1.520, $p = 0.2116$, $\eta p^2 = 0.115$). (G) Representative immunofluorescence images of TH^+ DA neurons in the mouse substantia nigra (scale bar: 320 μm). (H) Quantification of TH^+ DA neurons in the substantia nigra (n = 4) (One-way ANOVA, F (4, 15) = 3.450, $p = 0.0345$, $\eta p^2 = 0.479$). (I) Quantification of TH fluorescence intensity in the substantia nigra (n = 4) (One-way ANOVA, F (4, 15) = 3.159, $p = 0.0453$, $\eta p^2 = 0.457$). * $p < 0.05$, ** $p < 0.01$ vs Veh group in total distance moved. $^{\#}$ $p < 0.05$, $^{\#\#}$ $p < 0.01$ vs Veh group in center crossing times. MPTP, 1-methyl-4-phenyl-1,2,3,6-tetrahydropyridine; PD, Parkinson's disease; ANOVA, analysis of variance; DA, dopaminergic; TH^+, tyrosine hydroxylase-positive; Veh, vehicle; Cont, control; Mad, madopar; Sar-L, low-dose sarsasapogenin; Sar-H, high-dose sarsasapogenin; DAPI, 4′,6-diamidino-2-phenylindole.

and their mean fluorescence intensity in the Veh group compared with the Cont group (Fig. 1G). Administration of (Sar-H) and madopar significantly rescued the loss of TH^+ DA neurons in MPTP-induced PD mice (Fig. 1H,I).

Collectively, these results demonstrate that sarsasapogenin effectively ameliorates MPTP-induced hyperactive behaviors in PD mice, which may be associated with its protective role in preserving the survival of DA neurons.

3.2 Sarsasapogenin Modulates Neurotransmitter Expressions in MPTP-Induced PD Mice

Accumulating evidence indicates that the maintenance of key neurotransmitter homeostasis within the striatum and basal ganglia is critical for alleviating or delaying the progression of PD [23]. Subsequent to the behavioral assessments, deeply anesthetized prior to euthanasia. The midbrain was dissected and subjected to HPLC analysis to quantify the levels of monoamine neurotransmitters and their metabolites.

The results of neurotransmitter profiling are presented in Fig. 2. Compared with the Cont group, mice in the MPTP-treated vehicle group exhibited significantly reduced levels of NE and DA, increased levels of DOPAC and 5-HIAA, while no significant changes were observed in the levels of 5-HT and MHPG (Fig. 2A−K). Madopar significantly elevated NE and DA and reduced MHPG and 5-HIAA levels. In contrast, high-dose sarsasapogenin significantly increased DA and decreased MHPG levels, but it only showed an increasing trend toward NE. Notably, the Veh group exhibited significantly increased metabolite/neurotransmitter ratios (MHPG/NE, DOPAC/DA, and 5-HIAA/5-HT) compared with the Cont group, ratios that reflect neurotransmitter turnover efficiency. These elevated ratios which were significantly reversed by treatment with Madopar or sarsasapogenin, suggest that sarsasapogenin can normalize MPTP-disrupted neurotransmitter turnover (Fig. 2C,F,I).

3.3 Sarsasapogenin Inhibits Peripheral Inflammatory Response in MPTP-Induced PD Mice

Dopaminergic neurons are highly vulnerable to oxidative stress and inflammatory insults. Both cytokine/chemokine-induced cytotoxicity and excessive neuroinflammatory responses contribute to dopaminergic neuron degeneration and the progression of PD [24]. Neuroinflammation plays a pivotal role in the neurodegenerative pathogenesis of PD, which is characterized by microglial activation and upregulation of proinflammatory cytokines [25].

To evaluate the anti-inflammatory effects of sarsasapogenin in MPTP-induced PD mice, the serum concentrations of proinflammatory cytokines TNF-α, IL-1β, and anti-inflammatory cytokines IL-10, TGF-β were quantified using ELISA kits.

The results are presented in Fig. 3. Compared with the Cont group, the Veh group exhibited significantly elevated serum levels of the proinflammatory cytokines IL-1β and TNF-α, whereas the serum levels of the anti-inflammatory cytokines TGF-β and IL-10 remained unchanged (Fig. 3A−D). In contrast, treatment with Sar-H significantly downregulated the serum levels of TNF-α and IL-1β in PD mice, restoring them to near-normal levels. Sar-L showed significantly downregulated IL-1β and a trend toward reducing TNF-α levels. Neither dose of sarsasapogenin had a significant impact on the serum levels of IL-10 and TGF-β compared with the Veh group.

These findings demonstrate that sarsasapogenin exerts potent anti-inflammatory effects in MPTP-induced PD mice by specifically suppressing the peripheral secretion of proinflammatory cytokines, which may indirectly alleviate neuroinflammation-associated DA neuron damage.

3.4 Sarsasapogenin Attenuates MPP^+-Induced Primary Neuronal Neurite Atrophy

Accumulating evidence indicates that axon terminals are highly susceptible to exogenous and endogenous insults, undergoing degeneration during the early stages of PD [26]. Therefore, therapeutic strategies aimed at preventing synaptic terminal loss or promoting neurite outgrowth may alleviate the core pathological symptoms of PD. Primary neuronal cultures are widely used to investigate axonal outgrowth and neuronal protection due to their ability to recapitulate *in vivo* neuronal phenotypes [27]. Thus, the present study employed *in vitro* primary neuronal cultures to evaluate the effects of sarsasapogenin on neurite outgrowth in primary cultured neurons.

First, primary neurons were obtained from the cerebral cortex of E14 mouse embryos to establish an MPP^+-induced PD cell model. Compared to Cont cells, MPP^+ at 30–50 μM significantly reduced the viability of primary cortical neurons (Fig. 4A). To assess the effect of sarsasapogenin on MPP^+-induced axonal injury, primary neurons were co-incubated with 30 μM MPP^+ and sarsasapogenin (1 and 10 μM) for 2 days, followed by immunofluorescence staining with β3-tubulin and DAPI. The results demonstrated that sarsasapogenin significantly attenuated MPP^+-induced axonal atrophy, while exerting no significant effect on neuronal survival (Fig. 4B,C).

Next, primary ventral mesencephalic cultures were prepared from E14 mouse embryos. This method yields a mixed neuronal population, including DA, GABAergic, glutamatergic, and serotonergic neurons, as well as a small percentage of glial cells. No additional enrichment was performed, as the aim was to study DA neurons within their native cellular milieu, where cell-cell interactions may influence neuronal survival and neurite outgrowth, better mimicking the *in vivo* microenvironment. After 6 days of *in vitro* culture, immunofluorescence labeling with TH and MAP2 showed that TH^+ DA neurons accounted for 4.4%

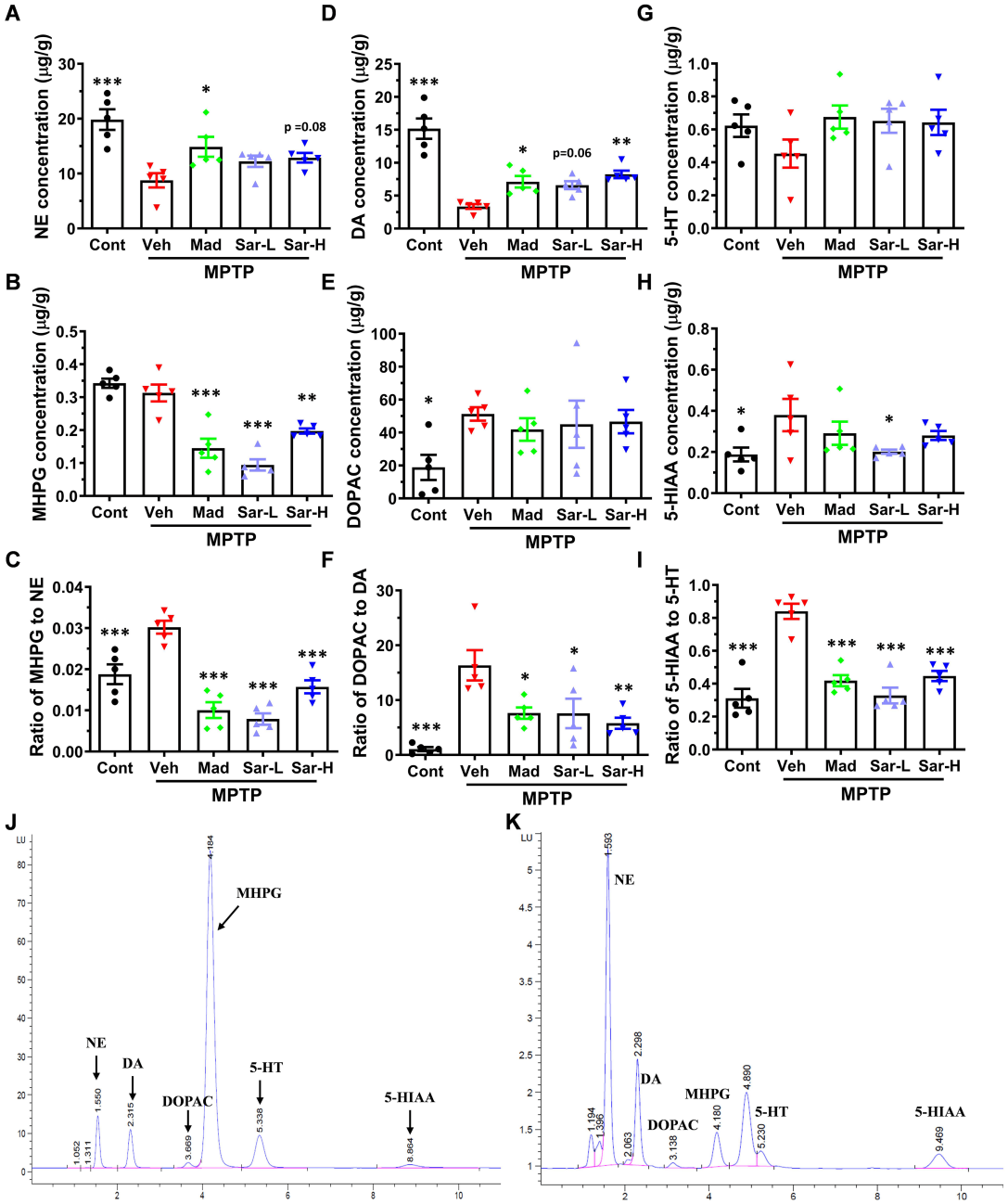

Fig. 2. Sarsasapogenin restores monoamine neurotransmitter homeostasis in the midbrain of MPTP-induced PD mice. Male C57BL/6 mice (3 months old) were intraperitoneally injected with MPTP (30 mg/kg) for 5 consecutive days to induce the PD model, followed by intragastric administration of low-dose sarsasapogenin (10 mg/kg, Sar-L), high-dose sarsasapogenin (20 mg/kg, Sar-H), or Madopar (50 mg/kg, Mad) for 21 consecutive days (n = 5). Midbrain was collected and measured by HPLC analysis. (A) NE concentration (One-way ANOVA, F (4, 20) = 6.228, $p = 0.0015$, $\eta p^2 = 0.520$). (B) MHPG concentration (One-way ANOVA, F (4, 20) = 12.61, $p < 0.0001$, $\eta p^2 = 0.687$). (C) MHPG/NE ratio (One-way ANOVA, F (4, 20) = 17.59, $p < 0.0001$, $\eta p^2 = 0.754$). (D) DA concentration (One-way ANOVA, F (4, 20) = 17.71, $p < 0.0001$, $\eta p^2 = 0.755$). (E) DOPAC concentration (One-way ANOVA, F (4, 20) = 1.990, $p = 0.1330$, $\eta p^2 = 0.275$). (F) DOPAC/DA ratio (One-way ANOVA, F (4, 20) = 6.822, $p = 0.0010$, $\eta p^2 = 0.554$). (G) 5-HT concentration (One-way ANOVA, F (4, 20) = 0.5504, $p = 0.7006$, $\eta p^2 = 0.087$). (H) 5-HIAA concentration (One-way ANOVA, F (4, 20) = 4.319, $p = 0.0094$, $\eta p^2 = 0.429$). (I) 5-HIAA/5-HT ratio (One-way ANOVA, F (4, 20) = 21.05, $p < 0.0001$, $\eta p^2 = 0.785$). (J) Chromatogram of a mixed standard solution of monoamine neurotransmitters and their metabolites. (K) Chromatogram of a representative sample. * $p < 0.05$, ** $p < 0.01$, *** $p < 0.001$ vs Veh group. HPLC, high-performance liquid chromatography; NE, norepinephrine; MHPG, 3-methoxy-4-hydroxyphenylglycol; DOPAC, dihydroxyphenylacetic acid; 5-HT, 5-hydroxytryptamine; 5-HIAA, 5-hydroxyindoleacetic acid.

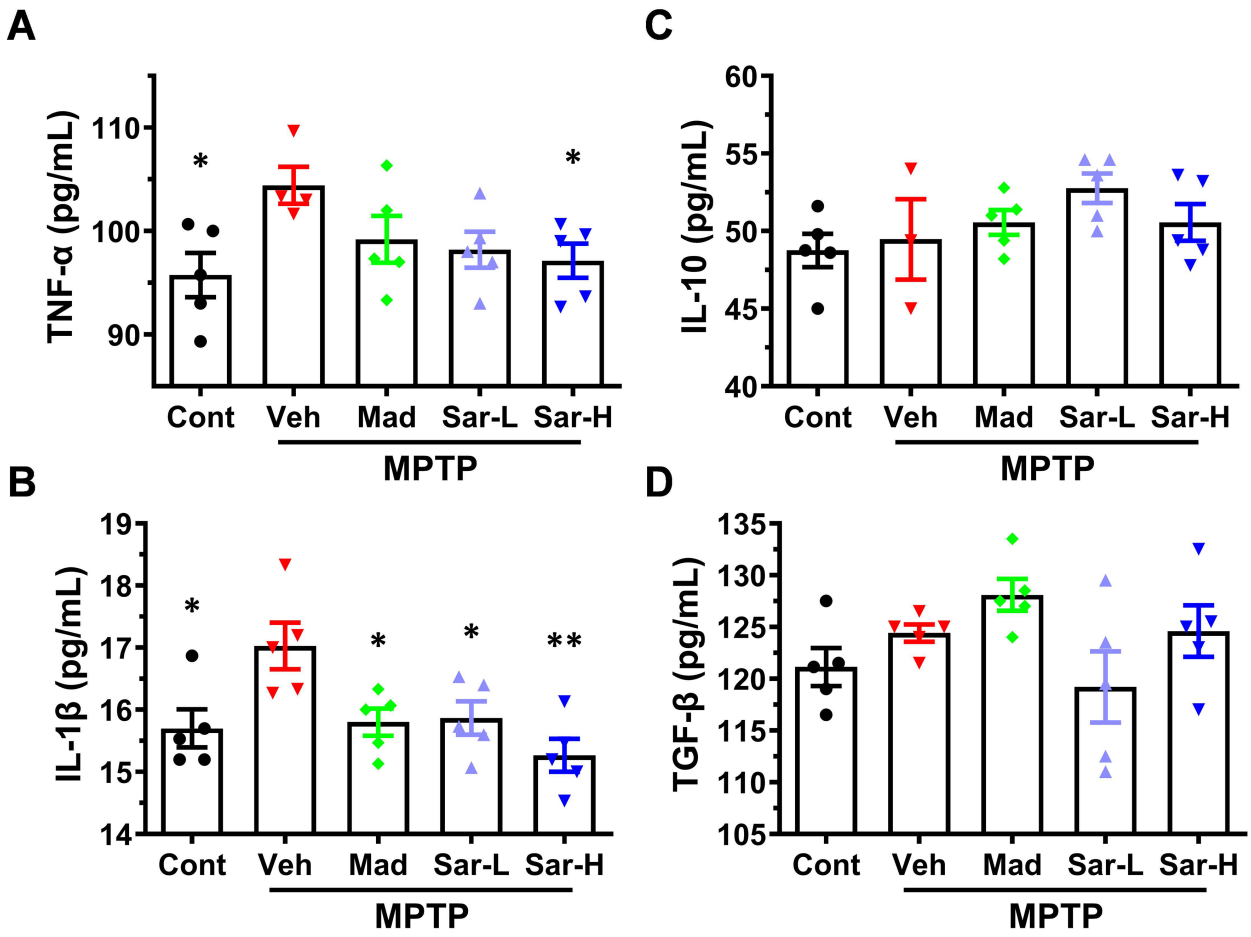

Fig. 3. Sarsasapogenin decreases peripheral proinflammatory cytokine levels in MPTP-induced PD mice. Male C57BL/6 mice (3 months old) were intraperitoneally injected with MPTP (30 mg/kg) for 5 consecutive days to induce the PD model, followed by intragastric administration of low-dose sarsasapogenin (10 mg/kg, Sar-L), high-dose sarsasapogenin (20 mg/kg, Sar-H), or Madopar (50 mg/kg, Mad) for 21 consecutive days. Serum was collected and measured by ELISA analysis (n = 5). (A) Serum level of TNF-α (One-way ANOVA, F (4, 20) = 1.875, $p = 0.1506$, $\eta p^2 = 0.254$). (B) Serum level of IL-1β (One-way ANOVA, F (4, 20) = 2.784, $p = 0.0519$, $\eta p^2 = 0.336$). (C) Serum level of IL-10 (One-way ANOVA, F (4, 20) = 1.155, $p = 0.3560$, $\eta p^2 = 0.167$). (D) Serum level of TGF-β (One-way ANOVA, F (4, 20) = 2.970, $p = 0.0409$, $\eta p^2 = 0.341$). * $p < 0.05$, ** $p < 0.01$ vs Veh group. ELISA, enzyme-linked immunosorbent assay; TNF-α, tumor necrosis factor-α; IL-1β, interleukin-1β; TGF-β, transforming growth factor-β.

of total $MAP2^+$ neurons (Fig. 5A–C). Subsequently, an MPP^+-induced primary DA neuron PD model was established. Compared with normal neurons, treatment with 10 and 50 μM MPP^+ significantly reduced the survival rate of $MAP2^+$ neurons (Fig. 5D). In contrast, treatment with 2 or 5 μM MPP^+ caused substantial damage to the neurites of TH^+ DA neurons without affecting overall neuronal viability, 10 and 50 μM MPP^+ resulted in complete death of all dopaminergic neurons. (Fig. 5D–F). Based on these results, 2 μM MPP^+ was selected as the optimal concentration for subsequent experiments to specifically evaluate neurite protection on DA neurons.

The therapeutic effects of sarsasapogenin on MPP^+-insulted DA neurons were further investigated (Fig. 6A). Immunofluorescence analysis showed that 2 days' exposure to 2 μM MPP^+ led to a significant reduction in both the number of TH^+ DA neurons and neurite density compared to the Cont group. Following co-culture of DA neurons with sarsasapogenin for 2 days exerted significant neuroprotective effects. Specifically, 10–1000 nM sarsasapogenin markedly inhibited MPP^+-induced DA neurite atrophy, as indicated by increased neurite density (Fig. 6B,C). We additionally examined the protective effects of sarsasapogenin pretreatment against MPP^+-induced DA neuron damage. DA neurons were pretreated with sarsasapogenin for 2 days, followed by co-incubation with 2 μM MPP^+ for an additional 2 days (Fig. 6D). Compared with the Cont group, MPP^+ exposure significantly induced DA neuron apoptosis and neurite atrophy. Pretreatment with sarsasapogenin at concentrations of 0.1–1000 nM dramati-

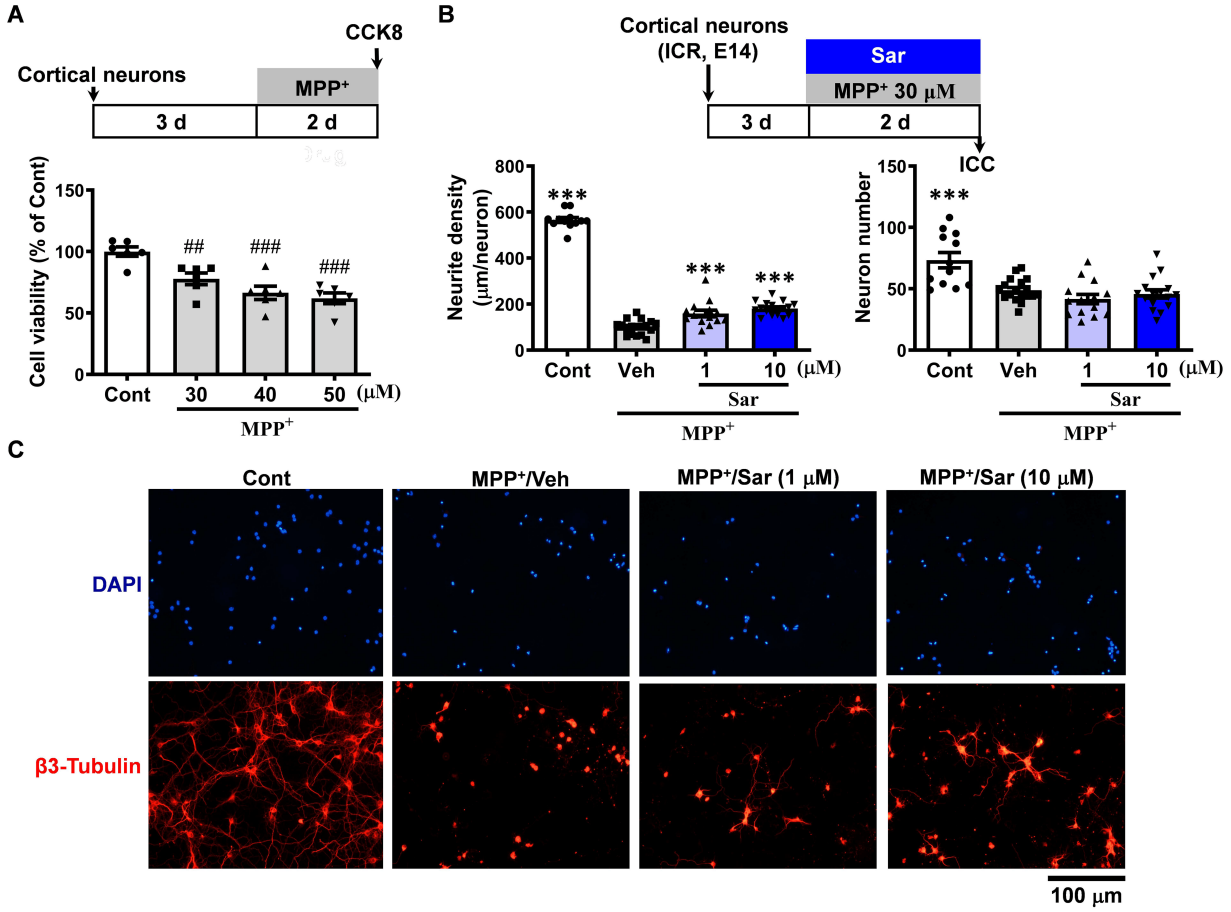

Fig. 4. Sarsasapogenin attenuates axonal atrophy in MPP$^+$-injured primary mouse cortical neurons. (A) Viability of primary cortical neurons treated with 30–50 μM MPP$^+$ for 2 days after 3 days of culture, determined by CCK-8 assay (n = 6) (One-way ANOVA, F (3, 20) = 13.45, $p < 0.0001$, $\eta p^2 = 0.669$), $^{\#\#}$ $p < 0.01$, $^{\#\#\#}$ $p < 0.001$ vs Cont. (B) Quantification of neurite density and neuronal number in primary cortical neurons co-treated with 30 μM MPP$^+$ and sarsasapogenin for 2 days after 3 days of pre-culture, assessed by immunofluorescence staining (n = 12–18 images, 8 embyos were used) (For neurite density, one-way ANOVA, F (3, 56) = 392.5, $p < 0.0001$, $\eta p^2 = 0.955$); (For one-way ANOVA, F (3, 56) = 12.02, $p < 0.0001$, $\eta p^2 = 0.392$), *** $p < 0.001$ vs Veh. (C) Representative β3-tubulin immunofluorescence images of primary cortical neurons (scale bar: 100 μm). MPP$^+$, 1-methyl-4-phenylpyridinium ion; CCK-8, Cell Counting Kit-8; ICR, Institute of Cancer Research; ICC, immunocytochemistry.

cally improved the survival rate of MPP$^+$-insulted DA neurons. Notably, 10–1000 nM sarsasapogenin significantly promoted the outgrowth of retracted neurites in MPP$^+$-damaged DA neurons (Fig. 6E,F).

Collectively, these *in vitro* findings demonstrate that sarsasapogenin exerts direct neuroprotective effects by inhibiting MPP$^+$-induced neurite atrophy in both cortical and DA neurons, and promotes neurite outgrowth in injured DA neurons, highlighting its potential as a therapeutic agent for PD.

3.5 Serpin H1 as the Target Candidate of Sarsasapogenin in Dopaminergic Neurons

To identify potential molecular targets of sarsasapogenin in DA neurons, we employed DARTS technology, a well-established method for screening small-molecule drug targets [28]. The underlying principle of DARTS is schematically illustrated in Fig. 7A. Briefly, upon binding to its target protein, a small-molecule induces conformational changes, that either stabilize the protein against protease-mediated degradation or render it more susceptible to hydrolysis. Following proteolysis, protein products are separated by SDS-PAGE, visualized by silver staining, and differentially expressed proteins between drug-treated and vehicle control groups are identified via nano LC-MS/MS [29,30]. This approach has been widely utilized for the identification of cellular targets of small-molecule compounds [31,32]. Combining DARTS with nano LC-MS/MS, we preliminarily identified Serpin H1 as a candidate molecular target of sarsasapogenin in DA neurons (Fig. 7B).

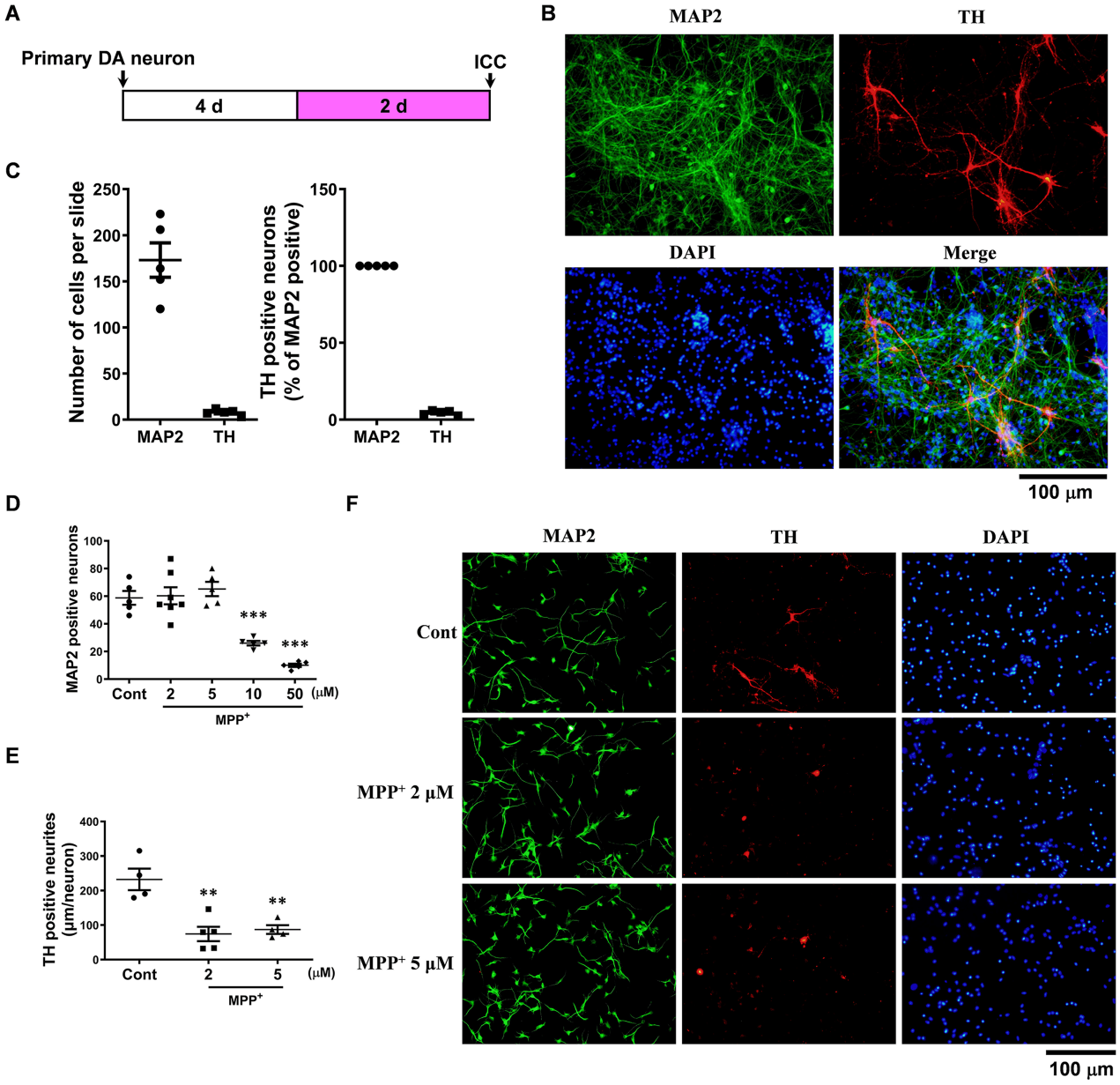

Fig. 5. MPP^+ induces dose-dependent axonal atrophy in primary mouse DA neurons. (A) Experimental workflow. Primary DA neurons isolated from E14 mouse embryos and immunofluorescence stained after 6 days of *in vitro* culture. (B) Representative immunofluorescence images of MAP2 and TH in primary DA neurons (scale bar: 100 μm). (C) Number of $MAP2^+$ and TH^+ cells per microscopic field, and the ratio of TH^+ to total $MAP2^+$ cells (n = 5). (D) Number of $MAP2^+$ neurons in primary DA neurons treated with 2–50 μM MPP^+ (n = 5–7) (One-way ANOVA, F (4, 18) = 16.63, $p < 0.0001$, $\eta p^2 = 0.787$). (E) Length of TH^+ neurites in primary DA neurons treated with 2–5 μM MPP^+ (n = 4–5) (One-way ANOVA, F (2, 9) = 12.73, $p = 0.0024$, $\eta p^2 = 0.739$). (F) Representative immunofluorescence images of $MAP2^+$ neurons and TH^+ neurites in primary DA neurons treated with 2–5 μM MPP^+ (scale bar: 100 μm). ** $p < 0.01$, *** $p < 0.001$ vs Cont. MAP2, microtubule-associated protein 2; Cont, control group.

To further assess the binding affinity and interaction mode between sarsasapogenin and Serpin H1, molecular docking simulations were performed. The 3D docking model revealed that sarsasapogenin forms one hydrogen bond with the aspartic acid (ASP) residue of Serpin H1, with a bond length of 2.8 Å (Fig. 7C), suggesting ASP as a key residue involved in ligand-receptor binding. Additionally, the docking simulation yielded a binding energy of −8.6 kcal/mol (Fig. 7D), a value indicative of a favorable predicted binding score between sarsasapogenin and Serpin H1. The surface binding model demonstrated that sarsasapogenin fits tightly into a hydrophobic cavity on the surface of Serpin H1, with its molecular structure well-anchored in the binding pocket, a conformation that

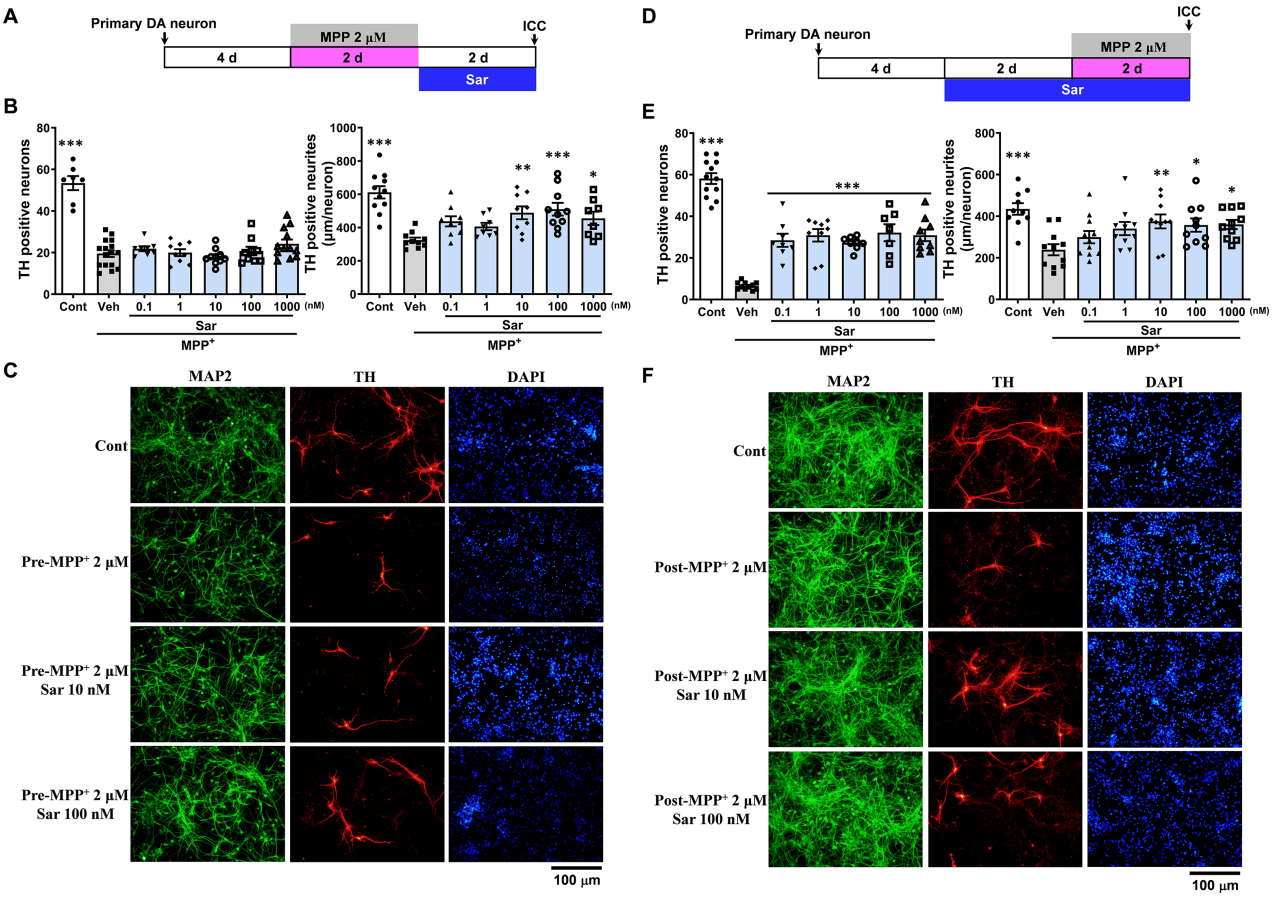

Fig. 6. Sarsasapogenin exerts protective effects on neurite outgrowth in MPP$^+$-insulted primary mouse DA neurons. (A) Experimental protocol for the therapeutic treatment. Primary DA neurons cultured for 4 days were treated with 2 μM MPP$^+$ for 2 days, followed by sarsasapogenin administration for an additional 2 days (8 embyos were used). (B) Number and neurite length of TH$^+$ primary DA neurons in the therapeutic treatment (n = 7–16 images) (For neuronal number, One-way ANOVA, F (6, 64) = 31.18, $p < 0.0001$, $\eta p^2 = 0.305$; for neuronal length, One-way ANOVA, F (6, 58) = 8.078, $p < 0.0001$, $\eta p^2 = 0.455$). (C) Representative immunofluorescence images of MAP2$^+$ neurons and TH$^+$ neurites in the therapeutic treatment (scale bar: 100 μm). (D) Experimental protocol for the preventive pretreatment. Primary DA neurons cultured for 4 days were pretreated with sarsasapogenin for 2 days, followed by co-treatment with 2 μM MPP$^+$ for an additional 2 days (8 embyos were used). (E) Number and neurite length of TH$^+$ primary DA neurons in the preventive pretreatment (n = 7–12 images, 8 embyos were used) (For neuronal number, One-way ANOVA, F (6, 65) = 42.89, $p < 0.0001$, $\eta p^2 = 0.796$; for neuronal length, One-way ANOVA, F (6, 65) = 4.517, $p = 0.0007$, $\eta p^2 = 0.294$). (F) Representative immunofluorescence images of MAP2$^+$ neurons and TH$^+$ neurites in the preventive pretreatment (scale bar: 100 μm). * $p < 0.05$, ** $p < 0.01$, *** $p < 0.001$ vs Veh group.

favors stable ligand-receptor interaction. The 2D interaction diagram further revealed that sarsasapogenin interacts with multiple amino acid residues of Serpin H1 via van der Waals forces, which are critical for maintaining the stability of the ligand-receptor complex. Moreover, sarsasapogenin forms π-alkyl hydrophobic interactions with histidine (His) residues of Serpin H1, which further enhance the binding affinity between the ligand and receptor (Fig. 7E). It is important to note that these findings are preliminary and require further validation to confirm the functional relevance of Serpin H1 as a target of sarsasapogenin. Thus, Serpin H1 should be considered a putative target of sarsasapogenin at this stage.

4. Discussion

Axonal degeneration is a pivotal pathological event in PD progression, and early synaptic dysfunction and loss are increasingly recognized as potential therapeutic targets for preventing disease onset and decelerating its progression [33]. PD-associated synaptic loss can be induced by α-synuclein aggregation formation, while axonal degeneration is a prominent consequence of DA neuron loss in the substantia nigra. Thus, protecting DA neurons is critical for maintaining physiological DA levels in the striatum and preserving motor coordination [26]. To date, no clinically established drugs or therapeutic approaches that can effectively reconstruct neural circuits in PD patients. A grow-

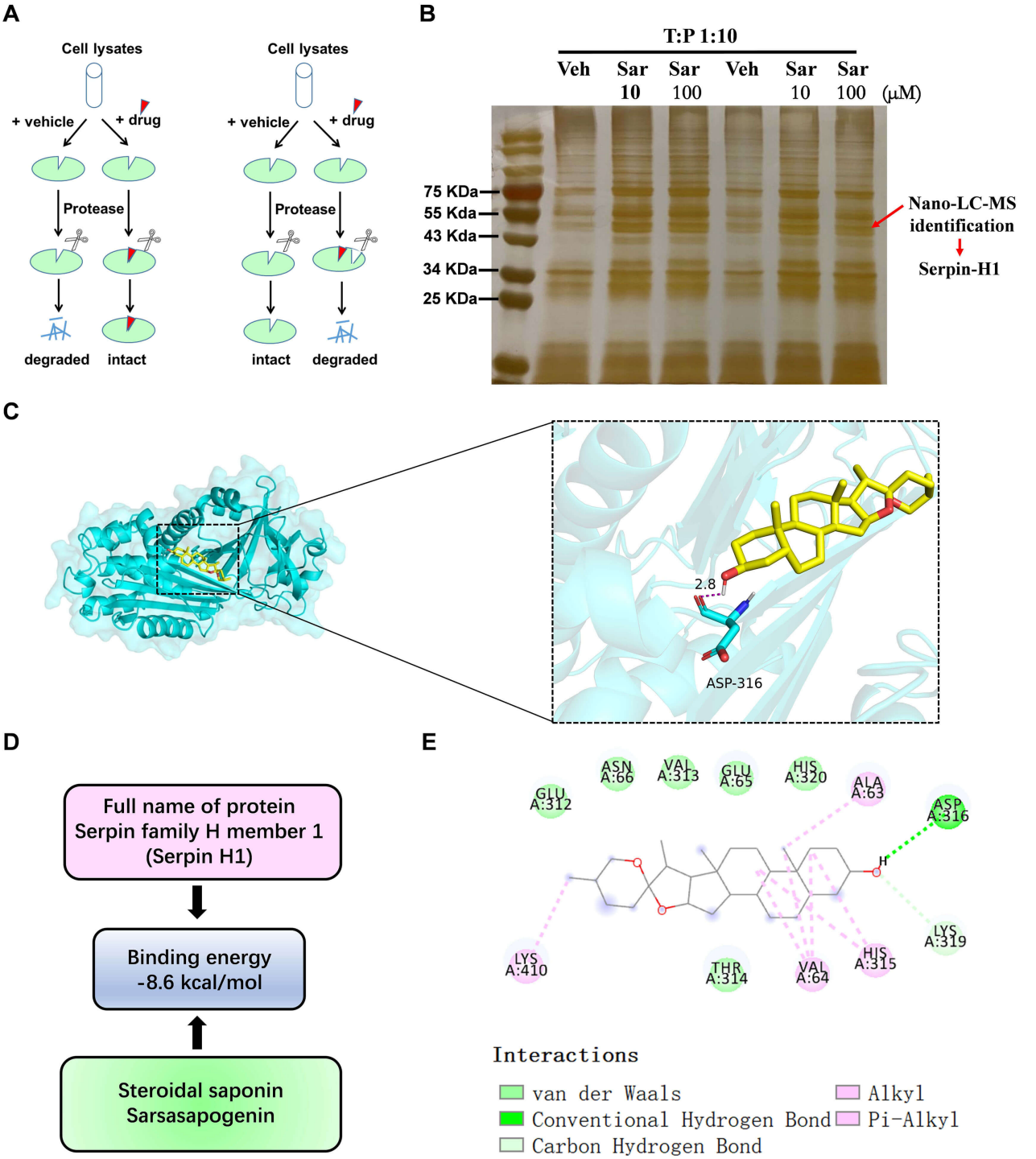

Fig. 7. Identification of Serpin H1 as a potential target of sarsasapogenin in DA neurons. (A) Schematic illustration of the DARTS principle. (B) Representative silver-staining image of the DARTS assay (two biological replicates). (C) 3D molecular docking model of sarsasapogenin bound to Serpin H1. (D) Molecular docking binding affinity of sarsasapogenin with Serpin H1. (E) 2D molecular interaction diagram of sarsasapogenin and Serpin H1. DARTS, Drug Affinity Responsive Target Stability; 3D, Three-dimensional; 2D, Two-dimensional.

ing body of evidence indicates that many naturally derived compounds exert multi-targeted neuroprotective effects in PD models, including anti-inflammatory, antioxidant, mitochondrial protective, anti-apoptotic, and neurotrophic effects [34,35]. Notably, these naturally derived compounds not only reduce neurotoxicity but also improve bioavailability and exhibit fewer adverse effects, making them promising alternative therapies for PD [36]. Furthermore, nat-

ural compounds have shown significant potential in promoting nervous system regeneration and neuroprotection [37]. Sarsasapogenin has been shown to exert distinct neuroprotective effects in preclinical studies of Alzheimer's disease [14,38]. In the present study, we extend these findings by demonstrating that sarsasapogenin harbors promising therapeutic potential for PD, as it modulates neurotransmitter homeostasis, suppresses excessive inflammatory responses, and promotes neurite protection and outgrowth in DA neurons.

MPTP is a well-established neurotoxin widely used to generate experimental models of PD. However, the behavioral consequences of subacute MPTP exposure remain variable and do not consistently reproduce the classical hypokinetic phenotype observed in human PD [17,22]. Previous research has indicated that the manifestation of motor dysfunction in acute and chronic MPTP models is strongly correlated with the extent of nigrostriatal lesioning, whereas subacute MPTP exposure is associated with widespread locomotor hyperactivity [39]. This discrepancy is thought to depend on multiple factors, including lesion severity, administration regimen, timing of behavioral assessment, dopaminergic and non-dopaminergic extrastriatal neural transmission, and the extent of compensatory neural mechanisms [40]. Notably, striatal DA levels show no direct correlation with motor behavioral performance in this subacute model, which renders the detection of MPTP-induced behavioral alterations challenging.

Consistent with these previous observations, subacute MPTP treatment in the present study significantly damaged DA neurons and reduced DA content, yet it did not induce typical motor deficits. Instead, MPTP-treated mice exhibited increased locomotor activity in the open field test and a trend toward prolonged fall latency in the rotarod test. This paradoxical hyperlocomotion has been described in certain subacute MPTP paradigms and is thought to reflect adaptive/compensatory responses within the nigrostriatal system rather than preserved or improved motor function [41]. One key compensatory mechanism is an increase in DA turnover. Indeed, we observed a significant elevation of the DOPAC/DA ratio in MPTP-treated mice, indicating accelerated DA metabolism. Similarly, the NE turnover ratio (MHPG/NE) was also increased. Elevated DA and NE turnover can temporarily sustain extracellular catecholamine levels and postsynaptic activation despite marked DA depletion, thereby maintaining or even exaggerating locomotor output. This interpretation is consistent with earlier reports that the nigrostriatal system possesses a strong compensatory capacity for DA loss, only when DA depletion exceeds 80–90% does decompensation occur, leading to overt motor deficits. In our subacute model, the degree of DA depletion was likely within the compensable range, which explains the absence of classical parkinsonian motor impairments and the presence of hyperactivity. Importantly, treatment with sarsasapogenin attenuated this abnormal hyperlocomotor phenotype while simultaneously preserving TH^+ DA neurons and restoring monoamine homeostasis. These findings suggest that the behavioral normalization induced by sarsasapogenin is associated with stabilization of dopaminergic function and neural circuit integrity, rather than nonspecific motor inhibition. Future studies using chronic MPTP or α-synuclein-based models are needed to assess whether sarsasapogenin can ameliorate genuine motor deficits.

Neurotransmitter imbalance is a central pathological feature of PD and is closely associated with both motor and non-motor symptoms. Degeneration of nigrostriatal DA neurons leads to DA depletion in basal ganglia circuits, disrupting motor control and contributing to classical symptoms such as bradykinesia, rigidity, and tremor [23,42]. Dopaminergic degeneration in PD is accompanied by imbalances in the metabolism of various neurotransmitters, which in turn trigger a series of pathological cascades. Accordingly, dopamine replacement therapy remains the cornerstone of current PD management [43]. In the present study, MPTP exposure induced marked disturbances in monoamine homeostasis, as reflected by reduced DA and NE levels together with altered metabolite profiles. Treatment with sarsasapogenin partially restored neurotransmitter balance and reduced abnormal turnover, suggesting a broader neuromodulatory effect beyond simple dopaminergic replacement. Such multi-target regulation may be therapeutically advantageous, as interventions that simultaneously preserve DA neurons and normalize interconnected neurotransmitter networks could provide more comprehensive symptomatic relief and potentially slow disease progression.

Neuroinflammation is increasingly recognized as a central driver of PD progression. Activated microglia, infiltrating peripheral immune cells, and elevated pro-inflammatory cytokines contribute to DA neuron vulnerability and dysfunction. Both innate and adaptive immune responses have been implicated in toxin-induced PD models and human disease. For instance, cluster of differentiation 4-positive ($CD4^+$) T cells mediate brain inflammation and neurodegeneration in an α-synuclein overexpression mouse model, and glial responses are key features in classical 6-hydroxydopamine (6-OHDA)-induced rat models of dopaminergic degeneration [44,45,46]. The persistent inflammatory environment exacerbates synaptic damage and neuronal vulnerability, thereby accelerating neurodegeneration. Consequently, modulating inflammatory signaling has emerged as a highly promising strategy for the treatment of PD. We demonstrated that sarsasapogenin significantly reduced the elevated peripheral levels of TNF-α and IL-1β induced by MPTP exposure. Although circulating cytokines do not directly represent central neuroimmune activity, peripheral inflammation is increasingly recognized to interact with the brain through blood-brain barrier dysfunction, humoral signaling, and immune cell traf-

ficking. Thus, the anti-inflammatory effects observed here may contribute, at least in part, to the neuroprotective actions of sarsasapogenin. Future studies should further investigate its effects on microglial activation, astrocyte reactivity, and inflammatory pathways within the nigrostriatal system.

In vitro, MPP^+ exposure induced marked structural impairment and reduced viability in both cortical and DA neurons. Treatment with sarsasapogenin significantly attenuated these alterations, indicating protective effects on neuronal survival and neurite integrity under toxic conditions. These findings provide preliminary evidence that modulation of neurite pathology may contribute to the therapeutic profile of sarsasapogenin in PD. Axonal degeneration is an early pathological hallmark of PD, and its underlying molecular mechanisms are distinct from those governing neuronal soma damage [7,47]. Targeting axonal outgrowth thus provides novel therapeutic avenues for PD prevention and treatment. The observed preservation of neurite architecture by sarsasapogenin may therefore have important implications for maintaining neuronal connectivity and function. Together with the *in vivo* protection of TH^+ neurons and restoration of monoamine homeostasis, these *in vitro* results further support sarsasapogenin as a multi-target neuroprotective candidate for PD.

Using DARTS combined with nano LC MS/MS, we preliminarily identified Serpin H1, (also known as Hsp47), as a candidate molecular target of sarsasapogenin in primary DA neurons. Serpin H1 is an endoplasmic reticulum-resident chaperone involved in collagen processing and the unfolded protein response (UPR) [48]. Emerging evidence indicates that Serpin H1 is upregulated in the substantia nigra of PD patients and in PD-related stress models, where it may modulate the inositol-requiring enzyme 1α (IRE1α)-X-box binding protein 1 spliced (XBP1s) branch of the UPR pathway [49,50]. It is important to note that the functional link between sarsasapogenin binding to Serpin H1 and downstream effects such as α-synuclein clearance or neurite outgrowth is currently hypothetical and remains to be experimentally validated. While we observed that sarsasapogenin improved neurite outgrowth and preserved DA neurons, and molecular docking suggested a favorable interaction with Serpin H1, these findings do not directly demonstrate that the neuroprotective effects are mediated by Serpin H1. Future studies are required to: (i) confirm direct binding using cellular thermal shift assay or surface plasmon resonance; (ii) determine whether Serpin H1 knockdown or overexpression modifies sarsasapogenin's neuroprotective activity; and (iii) examine whether sarsasapogenin modulates UPR/endoplasmic reticulum (ER) stress pathways via Serpin H1 in DA neurons.

Despite the promising efficacy of sarsasapogenin in promoting neurite outgrowth and protecting DA neuron survival in experimental PD models, several limitations of the present study should be acknowledged. First, histological analyses were not performed in a blinded manner, whereas behavioral assessments were fully blinded. The lack of blinding in histology may introduce potential bias, and future experiments will address this by having independent investigators conduct histological evaluations. Second, the subacute MPTP model reproduces dopaminergic injury but does not consistently recapitulate progressive motor deficits, which are key features of human PD. Therefore, additional studies in chronic and α-synuclein-based PD models are required to further define the therapeutic potential of sarsasapogenin. Finally, the identification of Serpin H1 remains exploratory and requires orthogonal validation using biochemical and genetic approaches.

5. Conclusions

In conclusion, the present study demonstrates that sarsasapogenin ameliorates key pathological features of PD by restoring monoamine neurotransmitter homeostasis, suppressing excessive peripheral pro-inflammatory responses, and protecting midbrain DA neurons by attenuating MPP^+-induced neurite atrophy and promoting neurite outgrowth. Additionally, we preliminarily identified Serpin H1 as a potential molecular target that may mediate the axonal outgrowth effects of sarsasapogenin in DA neurons. Overall, this work supports sarsasapogenin as a multi-target neuroprotective candidate for the development of disease-modifying therapies for PD.

Availability of Data and Materials

Data can be obtained by contacting the corresponding author.

Author Contributions

WD: Methodology, Investigation, Validation, Data analysis, Writing original draft. JH: Methodology, Investigation. WL: Investigation. YZ: Data analysis, Writing review & editing. YPZ: Data analysis, Writing review & editing. ZY: Supervision, Resources, Conceptualization, Writing review & editing, Funding acquisition. All authors contributed to editorial changes in the manuscript. All authors read and approved the final manuscript. All authors have participated sufficiently in the work and agreed to be accountable for all aspects of the work.

Ethics Approval and Consent to Participate

All animal experimental procedures were performed strictly according to the National Institutes of Health Guide for the Care and Use of Laboratory Animals and approved by the Institutional Animal Care and Use Committee (IACUC) of Guangdong Ocean University (GDOU-LAE-2023-004).

Acknowledgment

Thanks to all the peer reviewers for their opinions and suggestions.

Funding

This research was funded by Guangdong Basic and Applied Basic Research Foundation (grant number 2020A1515010779), Guangdong University Featured Innovation Program Project (2024KTSCX199), and the Sustainable Development Program of Shenzhen Science and Technology Major Program (KCXFZ20240903093925033).

Conflicts of Interest

The authors declare no conflicts of interest.

Supplementary Material

Supplementary material associated with this article can be found, in the online version, at https://doi.org/10.31083/JIN50683.

References

[1] Arjunan SP, Kumar DK. Techniques for assessment of parkinsonism for diagnosis and rehabilitation. Springer: Berlin, Germany. 2022. https://doi.org/10.1007/978-981-16-3056-9

[2] Su D, Cui Y, He C, Yin P, Bai R, Zhu J, et al. Projections for prevalence of Parkinson's disease and its driving factors in 195 countries and territories to 2050: modelling study of Global Burden of Disease Study 2021. BMJ (Clinical Research Ed.). 2025; 388: e080952. https://doi.org/10.1136/bmj-2024-080952

[3] Rizek P, Kumar N, Jog MS. An update on the diagnosis and treatment of Parkinson disease. CMAJ : Canadian Medical Association Journal = Journal De L'Association Medicale Canadienne. 2016; 188: 1157–1165. https://doi.org/10.1503/cmaj.151179

[4] Xu L, Pu J. Alpha-Synuclein in Parkinson's Disease: From Pathogenetic Dysfunction to Potential Clinical Application. Parkinson's Disease. 2016; 2016: 1720621. https://doi.org/10.1155/2016/1720621

[5] Koch JC, Bitow F, Haack J, d'Hedouville Z, Zhang JN, Tönges L, et al. Alpha-Synuclein affects neurite morphology, autophagy, vesicle transport and axonal degeneration in CNS neurons. Cell Death & Disease. 2015; 6: e1811. https://doi.org/10.1038/cddis.2015.169

[6] Amartumur S, Nguyen H, Huynh T, Kim TS, Woo RS, Oh E, et al. Neuropathogenesis-on-chips for neurodegenerative diseases. Nature Communications. 2024; 15: 2219. https://doi.org/10.1038/s41467-024-46554-8

[7] Burke RE, O'Malley K. Axon degeneration in Parkinson's disease. Experimental Neurology. 2013; 246: 72–83. https://doi.org/10.1016/j.expneurol.2012.01.011

[8] Kurowska Z, Kordower JH, Stoessl AJ, Burke RE, Brundin P, Yue Z, et al. Is Axonal Degeneration a Key Early Event in Parkinson's Disease? Journal of Parkinson's Disease. 2016; 6: 703–707. https://doi.org/10.3233/JPD-160881

[9] Yang Z, Zhang C, Li X, Ma Z, Ge Y, Qian Z, et al. Heterophyllin B, a cyclopeptide from Pseudostellaria heterophylla, enhances cognitive function via neurite outgrowth and synaptic plasticity. Phytotherapy Research : PTR. 2021; 35: 5318–5329. https://doi.org/10.1002/ptr.7212

[10] Deng J, Feng X, Zhou L, He C, Li H, Xia J, et al. Heterophyllin B, a cyclopeptide from Pseudostellaria heterophylla, improves memory via immunomodulation and neurite regeneration in i.c.v.Aβ-induced mice. Food Research International (Ottawa, Ont.). 2022; 158: 111576. https://doi.org/10.1016/j.foodres.2022.111576

[11] Yang Z, Song C, Ge YW, Tohda C. Editorial: Treatment of Alzheimer's disease-discovery of natural products based on neurite outgrowth and neuroprotection. Frontiers in Pharmacology. 2022; 13: 1079783. https://doi.org/10.3389/fphar.2022.1079783

[12] Mustafa NH, Sekar M, Fuloria S, Begum MY, Gan SH, Rani NNIM, et al. Chemistry, Biosynthesis and Pharmacology of Sarsasapogenin: A Potential Natural Steroid Molecule for New Drug Design, Development and Therapy. Molecules (Basel, Switzerland). 2022; 27: 2032. https://doi.org/10.3390/molecules27062032

[13] Huang C, Dong D, Jiao Q, Pan H, Ma L, Wang R. Sarsasapogenin-AA13 ameliorates Aβ-induced cognitive deficits via improving neuroglial capacity on Aβ clearance and antiinflammation. CNS Neuroscience & Therapeutics. 2017; 23: 498–509. https://doi.org/10.1111/cns.12697

[14] Zhang YM, Zheng T, Huang TT, Gu PP, Gou LS, Ma TF, et al. Sarsasapogenin attenuates Alzheimer-like encephalopathy in diabetes. Phytomedicine : International Journal of Phytotherapy and Phytopharmacology. 2021; 91: 153686. https://doi.org/10.1016/j.phymed.2021.153686

[15] Kong L, Liu Y, Zhang YM, Li Y, Gou LS, Ma TF, et al. Sarsasapogenin ameliorates diabetes-associated memory impairment and neuroinflammation through down-regulation of PAR-1 receptor. Phytotherapy Research. 2021; 35: 3167–3180. https://doi.org/10.1002/ptr.7005

[16] Yu YY, Cui SC, Zheng TN, Ma HJ, Xie ZF, Jiang HW, et al. Sarsasapogenin improves adipose tissue inflammation and ameliorates insulin resistance in high-fat diet-fed C57BL/6J mice. Acta Pharmacologica Sinica. 2021; 42: 272–281. https://doi.org/10.1038/s41401-020-0427-1

[17] Jackson-Lewis V, Przedborski S. Protocol for the MPTP mouse model of Parkinson's disease. Nature Protocols. 2007; 2: 141–151. https://doi.org/10.1038/nprot.2006.342

[18] Ayerra L, Abellanas MA, Basurco L, Tamayo I, Conde E, Tavira A, et al. Nigrostriatal degeneration determines dynamics of glial inflammatory and phagocytic activity. Journal of Neuroinflammation. 2024; 21: 92. https://doi.org/10.1186/s12974-024-03091-x

[19] Lundblad LK, Rinaldi LM, Poynter ME, Riesenfeld EP, Wu M, Aimi S, et al. Detrimental effects of albuterol on airway responsiveness requires airway inflammation and is independent of β-receptor affinity in murine models of asthma. Respiratory Research. 2011; 12: 27. https://doi.org/10.1186/1465-9921-12-27

[20] Zhao Y, Liu L, Han Y, Bai J, Du G, Gao Q. Simultaneous detection of 8 monoamine neurotransmitters in the different sections of rat brains by high performance liquid chromatography with fluorescence detection. Se Pu = Chinese Journal of Chromatography. 2011; 29: 146–151. https://doi.org/10.3724/sp.j.1123.2011.00146

[21] Muñoz-Manchado AB, Villadiego J, Romo-Madero S, Suárez-Luna N, Bermejo-Navas A, Rodríguez-Gómez JA, et al. Chronic and progressive Parkinson's disease MPTP model in adult and aged mice. Journal of Neurochemistry. 2016; 136: 373–387. https://doi.org/10.1111/jnc.13409

[22] Zhang QS, Heng Y, Mou Z, Huang JY, Yuan YH, Chen NH. Reassessment of subacute MPTP-treated mice as animal model of Parkinson's disease. Acta Pharmacologica Sinica. 2017; 38: 1317–1328. https://doi.org/10.1038/aps.2017.49

[23] Jamwal S, Kumar P. Insight Into the Emerging Role of Striatal Neurotransmitters in the Pathophysiology of Parkinson's

Disease and Huntington's Disease: A Review. Current Neuropharmacology. 2019; 17: 165–175. https://doi.org/10.2174/1570159X16666180302115032

[24] Tiwari PC, Pal R. The potential role of neuroinflammation and transcription factors in Parkinson disease. Dialogues in Clinical Neuroscience. 2017; 19: 71–80. https://doi.org/10.31887/DCNS.2017.19.1/rpal

[25] Liu TW, Chen CM, Chang KH. Biomarker of Neuroinflammation in Parkinson's Disease. International Journal of Molecular Sciences. 2022; 23: 4148. https://doi.org/10.3390/ijms23084148

[26] Mishra AK, Dixit A. Dopaminergic Axons: Key Recitalists in Parkinson's Disease. Neurochemical Research. 2022; 47: 234–248. https://doi.org/10.1007/s11064-021-03464-1

[27] Tönges L, Frank T, Tatenhorst L, Saal KA, Koch JC, Szego ÉM, et al. Inhibition of rho kinase enhances survival of dopaminergic neurons and attenuates axonal loss in a mouse model of Parkinson's disease. Brain : a Journal of Neurology. 2012; 135: 3355–3370. https://doi.org/10.1093/brain/aws254

[28] Lomenick B, Hao R, Jonai N, Chin RM, Aghajan M, Warburton S, et al. Target identification using drug affinity responsive target stability (DARTS). Proceedings of the National Academy of Sciences of the United States of America. 2009; 106: 21984–21989. https://doi.org/10.1073/pnas.0910040106

[29] Lomenick B, Olsen RW, Huang J. Identification of direct protein targets of small molecules. ACS Chemical Biology. 2011; 6: 34–46. https://doi.org/10.1021/cb100294v

[30] Pai MY, Lomenick B, Hwang H, Schiestl R, McBride W, Loo JA, et al. Drug affinity responsive target stability (DARTS) for small-molecule target identification. Methods in Molecular Biology (Clifton, N.J.). 2015; 1263: 287–298. https://doi.org/10.1007/978-1-4939-2269-7_22

[31] Chen F, Li C, Cao H, Zhang H, Lu C, Li R, et al. Identification of Adenylate Kinase 5 as a Protein Target of Ginsenosides in Brain Tissues Using Mass Spectrometry-Based Drug Affinity Responsive Target Stability (DARTS) and Cellular Thermal Shift Assay (CETSA) Techniques. Journal of Agricultural and Food Chemistry. 2022; 70: 2741–2751. https://doi.org/10.1021/acs.jafc.1c07819

[32] Derry MM, Somasagara RR, Raina K, Kumar S, Gomez J, Patel M, et al. Target identification of grape seed extract in colorectal cancer using drug affinity responsive target stability (DARTS) technique: role of endoplasmic reticulum stress response proteins. Current Cancer Drug Targets. 2014; 14: 323–336. https://doi.org/10.2174/1568009614666140411101942

[33] Gcwensa NZ, Russell DL, Cowell RM, Volpicelli-Daley LA. Molecular Mechanisms Underlying Synaptic and Axon Degeneration in Parkinson's Disease. Frontiers in Cellular Neuroscience. 2021; 15: 626128. https://doi.org/10.3389/fncel.2021.626128

[34] So YJ, Lee JU, Yang GS, Yang G, Kim SW, Lee JH, et al. The Potentiality of Natural Products and Herbal Medicine as Novel Medications for Parkinson's Disease: A Promising Therapeutic Approach. International Journal of Molecular Sciences. 2024; 25: 1071. https://doi.org/10.3390/ijms25021071

[35] Luo S, Zhang L, Wu X, Wang J, Li Q, Chen W, et al. Therapeutic potential of neuroprotective plant extracts in Parkinson's disease. Frontiers in Neuroscience. 2026; 20: 1813133. https://doi.org/10.3389/fnins.2026.1813133

[36] Roni MAH, Jami MABS, Hoque S, Hasibuzzaman MA, Banu KH, Rozina, et al. Clinically proven natural products in aid of treating parkinson's disease: A comprehensive review. Current Medicine. 2024; 3: 6. https://doi.org/10.1007/s44194-024-00033-w

[37] Freire MAM. Natural compounds in neuroprotection and nervous system regeneration: A narrative review. Regenerative Medicine Reports. 2026; 3: 115-123. https://doi.org/10.4103/REGENMED.REGENMED-D-25-00038

[38] Zhou M, Sun J, Yu Z, Wu Z, Li W, Liu G, et al. Investigation of Anti-Alzheimer's Mechanisms of Sarsasapogenin Derivatives by Network-Based Combining Structure-Based Methods. Journal of Chemical Information and Modeling. 2023; 63: 2881–2894. https://doi.org/10.1021/acs.jcim.3c00018

[39] Santoro M, Fadda P, Klephan KJ, Hull C, Teismann P, Platt B, et al. Neurochemical, histological, and behavioral profiling of the acute, sub-acute, and chronic MPTP mouse model of Parkinson's disease. Journal of Neurochemistry. 2023; 164: 121–142. https://doi.org/10.1111/jnc.15699

[40] Luchtman DW, Shao D, Song C. Behavior, neurotransmitters and inflammation in three regimens of the MPTP mouse model of Parkinson's disease. Physiology & Behavior. 2009; 98: 130–138. https://doi.org/10.1016/j.physbeh.2009.04.021

[41] Brotchie J, Fitzer-Attas C. Mechanisms compensating for dopamine loss in early Parkinson disease. Neurology. 2009; 72: S32–S38. https://doi.org/10.1212/WNL.0b013e318198e0e9

[42] Takeda A, Tomiyama M, Hanajima R. The Relationship Between Pathophysiology and Neurotransmitters in Parkinson's Disease. Brain and Nerve = Shinkei kenkyu no shinpo. 2021; 73: 829–837. https://doi.org/10.11477/mf.1416201843 (In Japanese)

[43] Aslan FS, Barut B, Ozturk S, Eyigurbuz T, Akyuz E. Neurotransmitter Dysregulation in Parkinson's Disease: Pathophysiological Insights and Therapeutic Perspectives. ACS Chemical Neuroscience. 2026; 17: 1432–1461. https://doi.org/10.1021/acschemneuro.5c00809

[44] Pajares M, I Rojo A, Manda G, Boscá L, Cuadrado A. Inflammation in Parkinson's Disease: Mechanisms and Therapeutic Implications. Cells. 2020; 9: 1687. https://doi.org/10.3390/cells9071687

[45] Williams GP, Schonhoff AM, Jurkuvenaite A, Gallups NJ, Standaert DG, Harms AS. CD4 T cells mediate brain inflammation and neurodegeneration in a mouse model of Parkinson's disease. Brain : a Journal of Neurology. 2021; 144: 2047–2059. https://doi.org/10.1093/brain/awab103

[46] Freire MAM, Rocha GS, Lemos NAM, Lima RR, Bittar S, Jenkins LB, et al. Insights into parkinson's disease pathology focusing on glial response and apoptosis in a classic rat model of dopaminergic degeneration. Neuroglia. 2025; 6: 36. https://doi.org/10.3390/neuroglia6030036

[47] Tagliaferro P, Burke RE. Retrograde Axonal Degeneration in Parkinson Disease. Journal of Parkinson's Disease. 2016; 6: 1–15. https://doi.org/10.3233/JPD-150769

[48] Ito S, Nagata K. Biology of Hsp47 (Serpin H1), a collagen-specific molecular chaperone. Seminars in Cell & Developmental Biology. 2017; 62: 142–151. https://doi.org/10.1016/j.semcdb.2016.11.005

[49] Bentea E, Verbruggen L, Massie A. The Proteasome Inhibition Model of Parkinson's Disease. Journal of Parkinson's Disease. 2017; 7: 31–63. https://doi.org/10.3233/JPD-160921

[50] Sepulveda D, Rojas-Rivera D, Rodríguez DA, Groenendyk J, Köhler A, Lebeaupin C, et al. Interactome Screening Identifies the ER Luminal Chaperone Hsp47 as a Regulator of the Unfolded Protein Response Transducer IRE1α. Molecular Cell. 2018; 69: 238–252.e7. https://doi.org/10.1016/j.molcel.2017.12.028